

# Application of quantum cascade lasers to trace gas detection

Z. BIELECKI<sup>1\*</sup>, T. STACEWICZ<sup>2</sup>, J. WOJTAS<sup>1</sup>, and J. MIKOŁAJCZYK<sup>1</sup>

<sup>1</sup> Institute of Optoelectronics, Military University of Technology, 2 Kaliskiego Str., 00-908 Warsaw, Poland

<sup>2</sup> Faculty of Physics at the University of Warsaw, 69 Hoża Str., 00-681 Warsaw, Poland

**Abstract.** The potential of Quantum Cascade Laser technology has been recently harnessed in industry, medicine and military to create a range of original infrared gas sensors. These sensors have opened up many new applications due to compact size, excellent sensitivity, robust construction and low power requirements. They rely on infrared absorption spectroscopy to determine identity and quantity of gases. The measurement of these gases has relied on different technologies including multi-pass spectroscopy, photoacoustic spectroscopy, cavity ring down spectroscopy, and their various modifications. In this review paper some technologies are described in terms of its advantages/disadvantages in many application. The results of own works about methane, ammonia, nitric oxide, nitrous oxide, and carbonyl sulfide detection are presented as well.

**Key words:** absorption spectroscopy, biomarkers sensors, gas sensors, cavity enhanced spectroscopy, photoacoustic spectroscopy.

## 1. Introduction

Detection of various gases and measurement of their concentration are very important for many human activities, starting from monitoring of industrial processes and investigation of their environmental impact, through searching of trace amounts of explosives to non-invasive medical diagnostics of various diseases by means of biomarkers concentration measurements in exhaled breath. Highly quantitative detection of gases is traditionally dominated by mass spectrometry, gas chromatography, pellistors, semiconductor gas sensors or electrochemical devices [1]. The main inconveniences of mass spectrometry and gas chromatography are the size and cost of the apparatus as well as the complicated maintenance. That causes an inability to make real-time on-line investigations. Pellistor gas sensors provide to measure the combustibility of the environment in which they are placed and to detect almost all combustible gases within explosive ranges [2]. A disadvantage of such sensors consists in zero drift at parts per million (ppm) levels. Semiconductor gas sensors also suffer from drift and moreover from cross-respond to other compounds and humidity levels [3]. Electrochemical sensors operate by reacting with the gas of interest and producing an electrical signal proportional to the gas concentration [4]. They can be relatively specific to individual gases and sensitive at ppm or ppb levels. However, they are also affected by limited lifetimes and some know cross-response issues, e.g. to humidity.

Laser absorption spectroscopy (LAS) is an effective tool for the detection of molecular trace gases. They offer fast responses (below 1 s), low drift, high gas selectivity and very high sensitivity, ranging from ppm and ppb to even ppt levels. That features depend strictly on properties of the species and the detection method [5]. This article provides a review of the breath analysis using the high sensitivity LAS.

## 2. Breath biomarkers

Exhaled air is a mixture of many gases. Beside main components of high concentration (nitrogen, oxygen, carbon dioxide, argon, water vapour) the traces of about 2000 compounds might be present in breath. Nitric oxide, ammonia, hydrogen and VOC's (Volatile Organic Compounds) are among them [6]. The origin of the molecules may be exogenous or endogenous. Exogenous molecules are inhaled from the environment and have no diagnostic value. Endogenous molecules are produced by the metabolic process in a human body. Then, these compounds are transported by blood and via the alveolar pulmonary membrane are exhaled with air. The concentration changes of trace molecules in an individual breath are related to a patient's diet, additions, stress level, immune status or the state of a health. That is why, the excess of concentration of some compounds might be a result of some diseases.

One of the generally accepted exhaled biomarkers is nitric oxide (NO). Its increased level might be associated with the occurrence of pulmonary inflammation and oxidative stress in various chronic lung ailment, including asthma and chronic obstructive pulmonary disease [7]. NO level in breath range from several ppb by volume to several hundred ppb. Measurements of carbon dioxide (CO<sub>2</sub>) concentration can be used to determine the dead space volume. These data are important for identification of the appropriate interval for NO measurement [8].

Another interesting breath compound is carbon monoxide (CO) that is a marker of oxidative stress. It is produced by the stress protein heme oxygenase and also by inflammation [9]. Increased levels of CO have been observed in asthmatics and in inflammatory airway diseases. Moreover, the test of exhaled carbon monoxide can detect neonatal jaundice.

\*e-mail: zbielecki@wat.edu.pl

Table 1  
Representative human breath biomarkers

Compound	Concentration	Physiological basis/pathology indication
Acetaldehyde	ppb	Ethanol metabolism
Acetone	ppm	Decarboxylation of acetoacetate, diabetes
Ammonia	ppb	Protein metabolism, liver and renal disease
Carbon dioxide	%	Product of respiration, <i>Helicobacter pylori</i>
Carbon disulfide	ppb	Gut bacteria, schizophrenia
Carbon monoxide	ppm	Production catalyzed by heme oxygenase
Carbonyl sulfide	ppb	Gut bacteria, liver disease
Ethane	ppb	Lipid peroxidation and oxidative stress, cancer
Ethanol	ppb	Gut bacteria
Ethylene	ppb	Lipid peroxidation, oxidative stress, cancer
Formaldehyde	ppm	Lung and breast cancer
Hydrocarbons	ppb	Lipid peroxidation/metabolism
Hydrogen	ppm	Gut bacteria
Isoprene	ppb	Cholesterol biosynthesis
Methane	ppm	Gut bacteria
Methanethiol	ppb	Methionine metabolism
Methanol	ppb	Metabolism of fruit
Methylamine	ppb	Protein metabolism
Nitric oxide	ppb	Production catalyzed by nitric oxide synthase
Oxygen	%	Required for normal respiration
Pentane	ppb	Lipid peroxidation, oxidative stress, cancer
Water	%	Product of respiration

Monitoring of ammonia concentration provides a fast, non-invasive diagnostics for patients with a variety of medical conditions, including liver and kidney disorders, and *Helicobacter pylori* infections [10].

Detection of carbonyl sulfide (OCS) is of importance in a number of applications which include not only medical diagnostics, but also atmospheric chemistry, industrial emission monitoring, and natural gas quality evaluation. Elevated OCS concentrations in the exhaled air have been observed in lung transplant recipients suffering from acute rejection as well as in patients with liver disease. The low ppb concentration of many volatile molecular species presents a complex challenge for clinical applications, which require rapid *in situ* detection of trace gases [11]. Exhaled ethane (C<sub>2</sub>H<sub>6</sub>) may indicate the oxidative damage to the body e.g. asthma, and chronic obstructive pulmonary disease. It is also correlated with rheumatoid arthritis, inflammatory bowel disease and deficiency in vitamin E for children [12, 13].

Acetone (C<sub>3</sub>H<sub>6</sub>O) is a very interesting biomarker for monitoring of blood glucose concentration for patients with diabetes mellitus, but also for searching of ventilation, cardiac output, physical exercises or ketonemia. The acetone concentration in healthy breath varies from 0.39 to 0.85 ppm [13].

Methane (CH<sub>4</sub>) is a biomarker of colonic fermentation and intestinal problems. The methane average concentration in normal human breath is in the range of about 3–8 ppm.

Lipid peroxidation can be diagnosed through analysis of breath ethylene (C<sub>2</sub>H<sub>4</sub>) and pentane (C<sub>5</sub>H<sub>12</sub>). Both might be correlated with cancer, however pentane is also the biomarker of schizophrenia.

Exhaled formaldehyde (CH<sub>2</sub>O) may be used as a marker for screening test for primary or metastatic lung cancer or breast cancer [14]. Its exhaled concentration for healthy men is about 0.3–0.6 ppm. In the case of breast cancer, it can reach even 1.2 ppm [15]. In Table 1, some representative human breath biomarkers are listed [9, 16].

### 3. Laser spectroscopic techniques for breath analysis

Laser absorption spectroscopy is of a great potential for detection and monitoring of constituents in gas phase. They combine high sensitivity and selectivity. In the simplest case – so called direct laser absorption spectroscopy (DLAS) – light beam of known intensity  $I_0$  and the wavelength  $\lambda$ , matched to the absorption line of the gas of interest, is directed through a gas sample cell. The amount of light  $I$  that is transmitted through the cell is registered by a detector. According to Lambert - Beer law the absorption coefficient  $\alpha(\lambda)$  is equal:

$$\alpha(\lambda) = \frac{1}{L} \ln \left( \frac{I_0(\lambda)}{I(\lambda)} \right), \quad (1)$$

where  $L$  denotes the optical path length. The coefficient  $\alpha(\lambda)$  is related to the absorption cross-section  $\sigma(\lambda)$  and the concentration of gas sample  $N$  by

$$\alpha(\lambda) = \sigma(\lambda)N. \quad (2)$$

Following Eq. (1) the detection limit ( $DL_{DLAS}$ ), is determined by

$$DL_{DLAS} = N|_{\min} \sigma(\lambda)L = \alpha_{\min}(\lambda)L$$

$$= \frac{I_0 - I}{I_0} = \frac{\Delta I}{I_0} \Big|_{\min} \quad (3)$$

Detection limit relies on the minimum detectable fractional change of the laser intensity. Any noise signal introduced by the light source, detection system or the optical path would deteriorate the sensitivity of the DLAS. Therefore the sensitivity of these techniques are usually limited to the range of  $10^{-2}$ – $10^{-4}$  [17], which is insufficient for trace gases detection.

The detection limit can be improved by the selection of a spectral range with the stronger absorption cross section. But choice of a strong absorption line at a unique wavelength for the selected species, preferably free of interference by other gases, is also important. This provides also high selectivity achievement. For many molecules of interest the strongest rotational-vibrational transitions are in the mid-infrared spectral region. The cross sections spectra are the functions of pressure and temperature while they are affected by pressure broadening, Doppler broadening and other effects. The parameters and procedures which might be found in standard databases like HITRAN provide opportunity for calculation of gases absorption cross-section [17]. At typical circumstances of breath analysis, i.e. at atmospheric pressure and at the room temperature the line corresponding to single ro-vibronic transition is described by Voigt profile of the width ( $\Delta\nu$ ) usually about 2–3 GHz [18]. Recent advances of quantum cascade lasers (QCL) and interband cascade ones (ICL) offer new attractive radiation sources for mid-infrared absorption spectroscopy with high spectral resolution and sensitivity [19].

Subsequently the improvement in the detection limit (3) can be achieved due to increase in signal-to-noise ratio. Wavelength modulation (WM) and frequency modulation spectroscopies (FMS) are the most common techniques used here. Both yield a lower detection limit of  $10^{-4}$ – $10^{-6}$  [13]. These methods are well applicable for tunable diode lasers absorption spectroscopy (TDLAS – WM/FM) due to good and ease spectral tunability of these light sources. Distributed feedback (DFB) lasers are especially useful for this purpose. An example of such experiment is presented in Fig. 1.

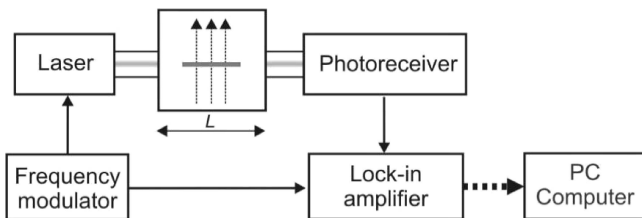


Fig. 1. Operation idea of TDLAS

The wavelength of probing laser is modulated over the absorption line by a sinusoidal signal of frequency  $f_m$ . Thereby the light intensity transmitted through the sample cell and the signal at the detector has the time-dependent form. The signal is detected with lock-in amplifier. Slow change of mean

laser frequency provides opportunity to register the first or the second derivative of the absorption spectrum, depending on demodulation frequency:  $f_m$  or  $2f_m$ , respectively.

Good selectivity and possibility of *in situ* measurements are the main advantages of TDLAS over DLAS approach. The WM or FM modulations are often combined with other methods of ultrasensitive laser absorption spectroscopy: multipass spectroscopy (MUPASS), cavity ring down spectroscopy (CRDS) or photoacoustic spectroscopy (PAS). MUPASS is based on lengthening of the effective light path due to placing of the sample between the mirrors (Fig. 2). The light beam is multiply reflected between the mirrors. That leads to increase the effective path-length even to 2 orders of magnitude. Multipass cells might be of Herriott or White construction, depending on their geometry. Thus the detection limit of the TDLAS-WM/FM technique combined with MUPASS cells can be as low as  $10^{-7}$ .

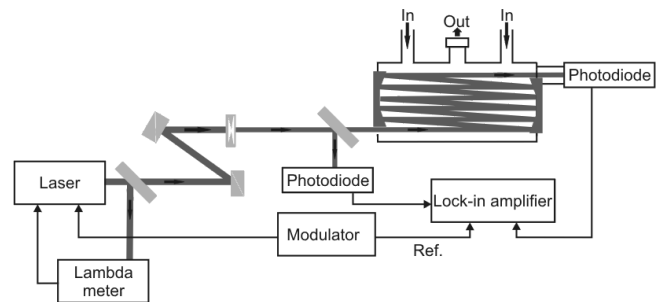


Fig. 2. Typical setup of MUPASS system

In the CRDS setup, optical cavity (resonator), which is usually built of two mirrors characterized by the very high reflectivity ( $R \rightarrow 1$ ) is employed (Fig. 3) [20–22]. Laser pulse is injected into the cavity through one of the mirrors.

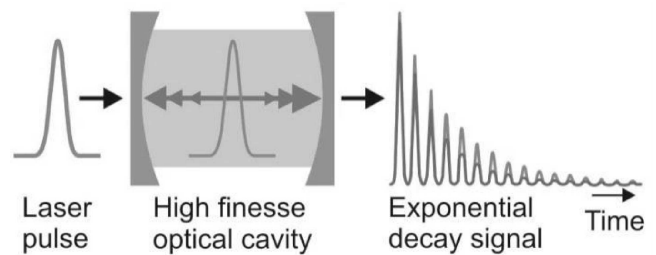


Fig. 3. Idea of the CRDS

Neglecting diffraction phenomena, the cavity losses occur due to residual transmission of the mirrors ( $T = 1 - R$ ) and the extinction in the medium filling the resonator ( $\alpha(\lambda)$ ). That causes exponential decay of radiation which is described by:

$$I(t) = I_0 e^{-\left[\frac{(1-R) + \alpha(\lambda)L}{L}c\right]t} = I_0 e^{-\frac{t}{\tau_A}}, \quad (4)$$

where  $\tau_A$  denotes the decay time

$$\tau_A = \frac{L}{c[(1-R) + \alpha(\lambda)L]} \quad (5)$$

and  $c$  is the light speed. Decay of the radiation can be observed by a photoreceiver located at the output mirror.

Calibration of the system is done for cavity without absorbing species ( $\alpha = 0$ ). In this case the formula (5) takes the form

$$\tau_0 = \frac{L}{c(1-R)}. \quad (6)$$

Comparing both decay times the absorber concentration can be found

$$N = \frac{1}{c\sigma(\lambda)} \left( \frac{1}{\tau_A} - \frac{1}{\tau_0} \right). \quad (7)$$

The detection limit is given by

$$DL_{CRDS} = N|_{\min} \sigma(\lambda) L = (1-R) \frac{\Delta\tau}{\tau_0} \Big|_{\min}. \quad (8)$$

In this case the detection limit relies on the minimum detectable fractional change of the decay time determination, which usually reaches the value of  $10^{-3}$ . Using cavity mirrors of very high reflectivity  $R$  (often exceeding 99.995%), the detection limit better than  $10^{-8}$  can be obtained.

The advantage of CRDS over other ultrasensitive absorption spectroscopy approaches consists not only in dominant sensitivity. As far as this technique is based on determination of resonator Q-factor (by means of decay time measurement or other method [23]), its superiority also results from minimizing impacts of light source intensity fluctuations or detector sensitivity changes.

It should be pointed out that the phenomena described by the formulas (4–8) take place only when the laser light is resonantly coupled to the cavity modes. Moreover the performance of the spectroscopy requires that the cavity mode is well coupled to peak of the absorption line of interest. Frequencies of neighbouring modes are separated by, so called, free spectral range (FSR):  $\Delta\nu_{FSR} = c/2L$ . Its value reaches 300 MHz for typical cavity length of 0.5 m. While for molecular lines broadened by collisional processes in air  $\Delta\nu_{FSR} \ll \Delta\nu$ , usually the absorption profile overlaps many modes. Finesse of the resonator [18]:

$$F = \frac{\Delta\nu_{FSR}}{\delta\nu} = \frac{\pi\sqrt{R}}{1-R}, \quad (9)$$

provides opportunity to determine the mode width  $\delta\nu$ . For  $R = 99.995\%$ ,  $F$  value is about 4.8 kHz. The linewidth of pulsed lasers is usually of several gigahertz or larger, then in the experiment with such light sources a part of their radiation couples well to many cavity modes.

But the best results of trace gas detection are achieved with *cw* single mode lasers. The use of such lasers in CRDS is possible due to AM modulation of the light beam. The detection limit below  $10^{-9}$  can be obtained with this method [24]. Free running *cw* distributed feedback diode (DFB) lasers provide the linewidths in the MHz range which is much less than the absorption linewidth  $\Delta\nu$ . Therefore these lasers can be precisely tuned to the peak of selected ro-vibronic transitions which ensures exact of absorption measurement. However using of the narrow band lasers for CRDS requires synchronization of cavity mode with their radiation. In the simplest case that is done by dithering of one of the mirrors by a piezoelement. That induces a variation of resonator mode frequencies and causes their random coincidence with laser line. For

ultrahigh sensitivity and precision an active locking of selected cavity mode with laser frequency is performed. Optical or electronic feedback is used in these applications [25–27].

There are several modifications of CRDS. One of them is cavity enhanced absorption spectroscopy (CEAS) technique. Due to off-axis introduction of laser beam to the cavity, the reflected light is spatially separated into  $k$ -beams inside the cavity. Factor  $k$  is the number of the laser beam trips. Free-spectral range for such off-axis arrangement can be  $k$  times less than the FSR for on-axis one. Due to that, either the dense mode structure of low finesse occurs or the mode structure does not establish at all. In this way, sharp resonances of the cavity are avoided, so the problem with laser modes and narrow absorption lines matching does not occur [28].

Powerful technique for detection of molecular compounds in gas phase is combination of locked CEAS with frequency modulation spectroscopy. This technique is called noise-immune cavity-enhanced optical-heterodyne molecular spectroscopy (NICE-OHMS). The laser frequency is electronically locked to a mode of the cavity to ensure a large cavity transmission. Modulation frequency is then imposed to the laser beam to produce frequency sidebands which are separated from the carrier by value of FSR. The radiation passes unchanged through the cavity unless an absorbing medium is present. In that case the cavity amplified FMS signal is produced (Fig. 4) [18]. FMS is used for reduction  $1/f$  noise, while CEAS – for increase in the interaction length between the light and the sample [17]. This technique can reach the detection limit of about  $10^{-13}$ . Thus such approach is of larger potential than any other method for trace gas analysis.

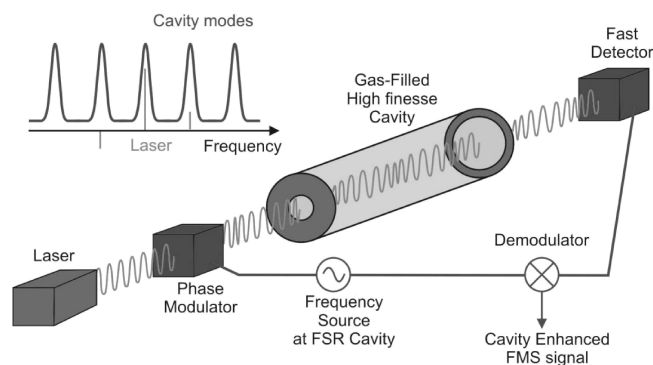


Fig. 4. Idea of the NICE-OHMS detection system

Other modifications of CRDS technique are integrated cavity output spectroscopy (ICOS) and cavity leak-out absorption spectroscopy (CALOS). The difference between these setups and CRDS is, that e.g. ICOS compares the integrated output of light intensities for two cases: with (case  $I_1$ ) and without absorption ( $I_0$ ) of the species in the gas cell. Then the absorption coefficient is determined from

$$\sigma(\lambda)L = (1-R) \frac{I_0 - I_1}{I_0} = (1-R) \frac{\Delta I}{I_0}. \quad (10)$$

This method is based upon the excitation of a dense spectrum of transverse cavity modes and then the signal averaging of the cavity output. It relies on the accidental coincidence

of the frequencies associated with laser and the cavity. The laser spectrum is repeatedly swept across one or several cavity modes. However, for high finesse cavities the ratio of “on” and “off” cavity modes is low, whereby the transmission as well as the integrated absorption becomes low. By dithering of one of the cavity mirrors the number of excited cavity modes can be increased.

In off-axis ICOS setup, an increase in spectral density of cavity modes is provided. Additionally, the cavity path length is growth about  $F/\pi$  times (where  $F$  is the cavity finesse) and the noise is minimized. In this setup geometry all transverse modes contribute to detection of the intra-cavity trace gas absorber. In comparison with CRDS and on-axis ICOS, this technique is insensitive to vibrations and misalignments, and can typically reach the detection limit of about  $10^{-7}$  [29]. The differences between on-axis alignment and off-axis one are shown in Fig. 5 [30].

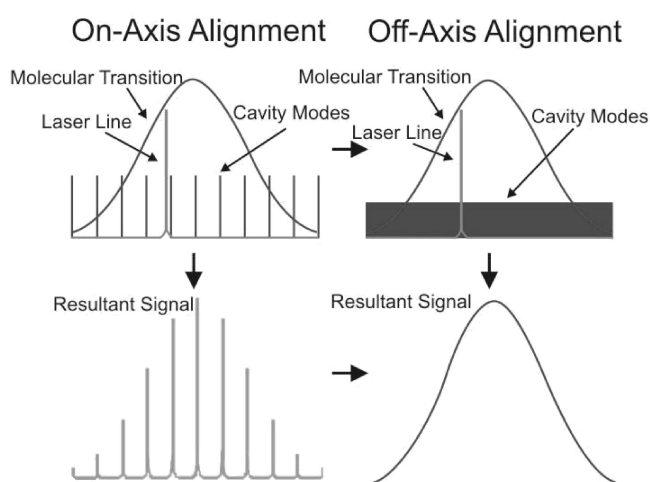


Fig. 5. Mode spectra on-axis alignment and off-axis one

CALOS is another cw variant of CRDS. The sensor is based on a laser and high-finesse cavity. After excitation, the laser power is turned off and the subsequent decay of the radiation stored in the cavity is observed via detection of the light leaking out through one of the cavity mirrors. Measurement of the decay time is used to determine the photon losses and thus to detect weakly absorbing species inside the cavity [31]. D. Halmer et al. observed a noise-equivalent absorption coefficient of  $7 \cdot 10^{-11} \text{ cm}^{-1} \text{ Hz}^{-1/2}$  using a cavity of 0.5 m length with  $R > 0.9999$  mirrors. In that setup, a detection limit of 7 ppt for carbonyl sulfide in ambient air was achieved [32].

Photoacoustic spectroscopy consists in conversion of a light energy into an acoustic wave [33]. When the modulated light is absorbed in the medium, the gas temperature is periodically changed and the acoustic wave with modulation frequency occurs (Fig. 6). The wave is detected using ultrasensitive microphone [34]. The sensitivity is increased by

using a cell in the form of acoustic resonator. The frequency of light modulation is matched close to this resonance.

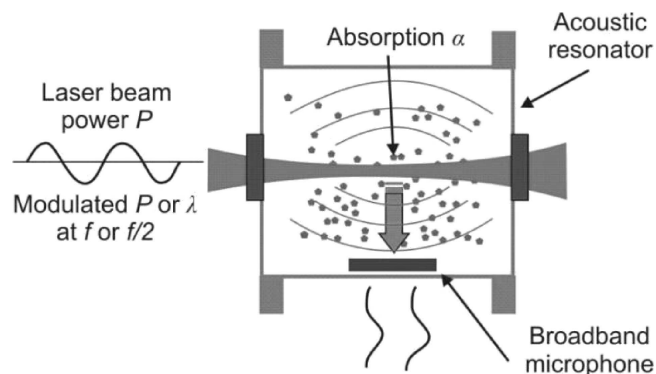


Fig. 6. Idea of photoacoustic spectroscopy

Among the so-called *in-situ* methods, PAS belongs to the most popular one. The absorber concentration in the investigated sample influences on the level of photoacoustic signal. Its amplitude registered by the microphone is given by

$$A(T, \lambda) \propto P_o N \alpha(T, \lambda) L \frac{m}{f_m V} \eta, \quad (11)$$

where  $P_o$  denotes average laser power,  $m$  is the modulation coefficient of radiation,  $f_m$  is the frequency of modulation,  $V$  is the gas volume, and  $\eta$  is the microphone efficiency. The sensitivity of the PAS is about several ppb.

There are several variants of photoacoustic approach. One of them is quartz enhanced photoacoustic spectroscopy (QEPAS) in which a special fork quartz oscillator as an acoustic wave sensor is applied [35]. The laser beam passes among bars of the fork. The receiver registers only the asymmetric oscillations of both bars that are caused by the light absorption in the investigated medium. Symmetric vibrations, which follow from external acoustic noises, provide the electric signals which are quenched in the sensor. Such solution increases the sensitivity of photoacoustic methods by two orders of magnitude. Moreover, QEPAS cells are characterized by a volume of several cubic centimetres only.

A novel approach to PAS was presented recently [36]. The photoacoustic cell was placed inside the optical resonator. The QCL wavelength ( $10.4 \mu\text{m}$ ) was coupled precisely to the cavity mode within whole tuning range ( $2.5 \text{ cm}^{-1}$ ). Due to light storage effect in the cavity, radiation power  $P_o$  was build up inside the photoacoustic cell about 181 times in comparison with nominal value of laser output power. Using this system the trace detection of ammonia at the level of 10 ppt is expected.

Figure 7 shows selected absorption techniques sorted by their sensitivity and complexity [17]. The font size symbolizes their current importance for trace detection of species.

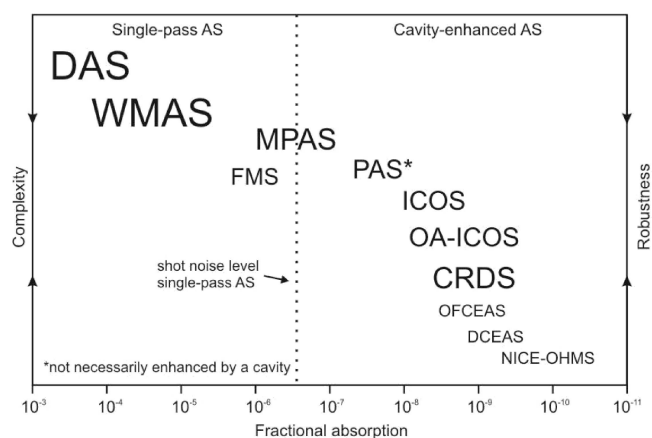


Fig. 7. Selected absorption techniques sorted by their sensitivity and complexity (where FMS means frequency modulation spectroscopy, OF-CEAS stands for optical – feedback cavity enhanced absorption spectroscopy and DCEAS denotes direct CEAS)

## 4. Experimental results

Laser spectroscopy methods can reach superior detection limits and in many cases they provide the opportunity to registration trace gases concentration even at ppt level. However their performances of biomarkers detection for medical application is limited when detecting the breath compounds by various interfering gases which are presented in the exhaled air. Mainly  $\text{H}_2\text{O}$  and  $\text{CO}_2$  are the most interfering species since they occur at concentrations reaching level of even 5% of the exhaled air.

**4.1. NIR measurement.** In Fig. 8 the absorption spectrum of  $\text{H}_2\text{O}$  and  $\text{CO}_2$  in visible and NIR range is presented. As one can see, majority of the spectrum is screened by absorption of these molecules. The observation of other compounds with sensitivity  $\alpha < 10^{-6} \text{ cm}^{-1}$  is possible only within several specific ranges, so called “atmospheric windows”, Therefore, an important matter is to search spectral regions and spectral line for which such interferences are minimized. From other point of view several compounds occur in the exhaled air in relatively high concentration. That concerns methane, which might be present in breath of healthy man with mixing ratio of 10 ppm [13], ammonia (2 ppm [13]), CO (10 ppm [37]) and acetone (1.4 ppm [38]). The high concentrations lead to the absorption coefficients exceeding the level of  $10^{-6} \text{ cm}^{-1}$ . Therefore the LAS setups for these species investigation might be of relatively low sensitivity. However their high selectivity to other compounds ought to be retained.

Some solutions of these problems might be performed within VIS – NIR. Ro-vibronic molecular lines usually correspond to overtone transitions there. Therefore their strengths are usually much lower than that one of the main oscillation frequencies located in MIR. Nevertheless combining these cross sections with high concentrations of selected molecules provides the absorption coefficient exceeding often the limit of  $10^{-6} \text{ cm}^{-1}$ . Moreover the apparatus that is built for VIS – NIR radiation might be relatively cheap and easy to construct due to wide availability of lasers (single mode DFB tunable

diode lasers), wavelength meters, photodetectors, electro-optic and acousto-optic modulators, fiber optic equipment as well as the filters and optic materials for lenses, prism etc. A test of this approach was a goal of our experiment.

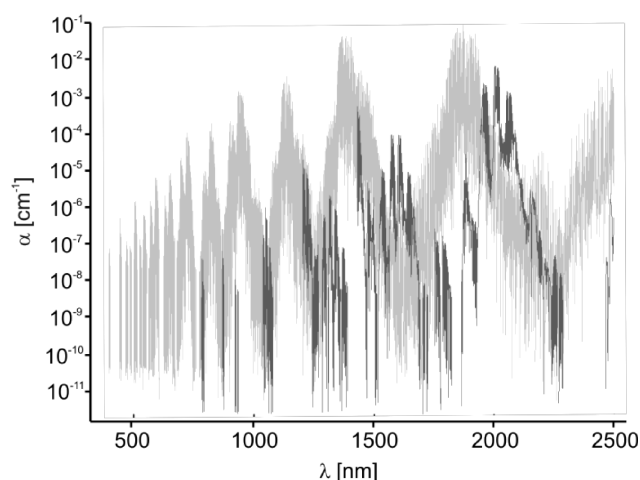


Fig. 8. Absorption spectra of  $\text{H}_2\text{O}$  (5%, bright line) and  $\text{CO}_2$  (5%, dark line) in the air

Our preliminary investigation was performed with methane. Comparison of its spectra with main breath interfering gases was presented in Fig. 9a. This region corresponds to, so called,  $\text{H}_2\text{O} - \text{CO}_2$  window i.e. minimum absorption, which provides opportunity to register the species within the range of absorption coefficients up to  $10^{-9} \text{ cm}^{-1}$ . The methane line of about 2253 nm is the best for detection of this compound. In Fig. 9b the absorption line of interest is presented. While our experiment was performed with wavelength modulation technique the modulation range was presented as well.

The experimental setup is presented in Fig. 10. DFB single model diode laser (Toptica, 5 mW) was tuned to the peak of 2253.6598 nm methane line with precision of 0.001 nm by means of a lambdameter (HighPrecision). Its wavelength was varied periodically on wing of the line (see Fig. 9b) using triangle current signal from a modulator. Synchronous rectangular reference signal was also provided to lock-in voltmeter. The main part of the laser beam was directed to photoacoustic cell. The frequency of modulation was close to acoustic resonance one (1930 Hz). The cell was filed with filtered air containing about 0.5% of  $\text{H}_2\text{O}$ . The admixture of 5% of  $\text{CO}_2$  and regulated amount of methane was added to the air in order to simulate human breath. Mixture composition was regulated by means of Beta-Erg flow controllers. Photoacoustic signal occurring at frequency of modulation was registered by a microphone and directed through the switch to lock-in amplifier (SRS model 830).

In the case of multipass measurement the laser beam was directed to the cell constructed with two mirrors of 5 m curvature radius, 0.5 m apart. Due to multiply reflection the effective path length in the cell was about 15 m. Signal intensity was monitored by two photodiodes (Thorlabs). One of them was used for measurement of light intensity, the second one

for detection of wavelength modulated signal that occurred in the cell. Both were recorded with lock-in amplifier at frequency of modulation.

Figure 11 shows measurement of methane concentration in the air with photoacoustic method (a) and multipass approach (b).

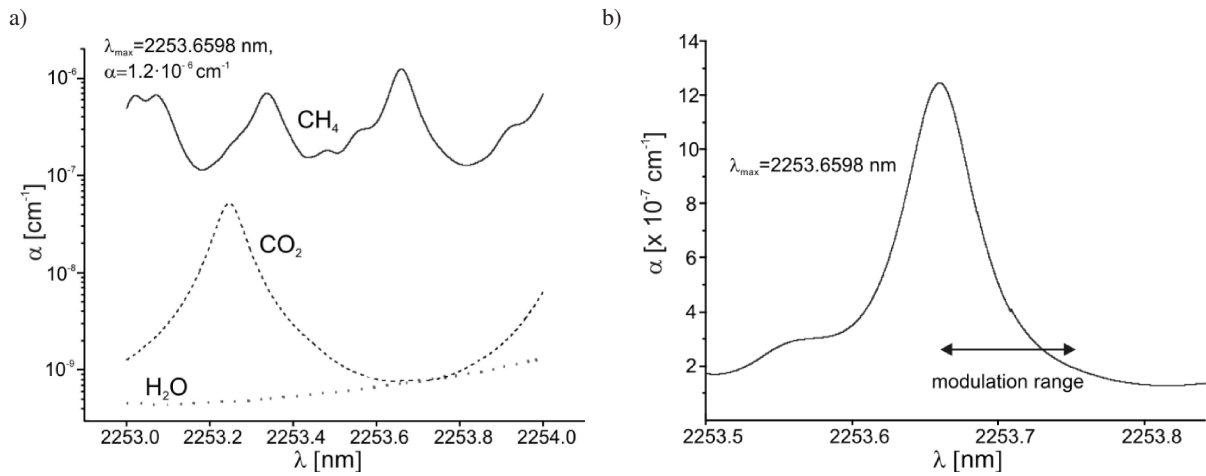


Fig. 9. Comparison of absorption spectrum of methane (10 ppm) with  $\text{H}_2\text{O}$  (5%) and  $\text{CO}_2$  (5% line) in air (a); absorption line of methane with wavelength modulation range (b)

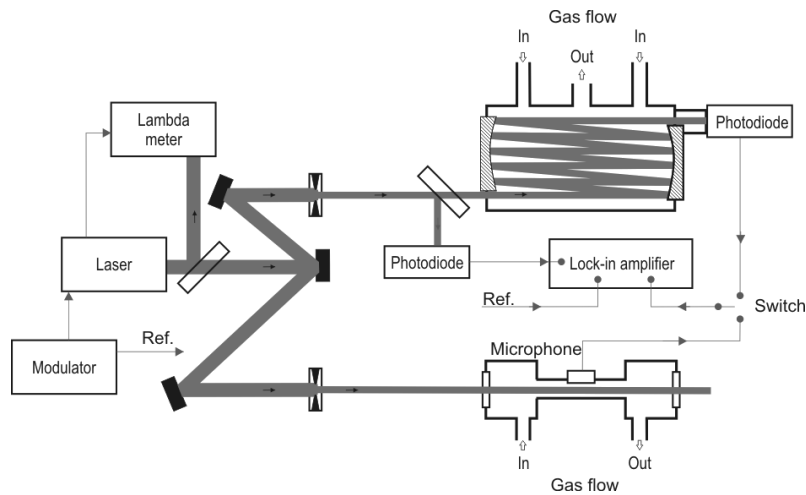


Fig. 10. Experimental setup

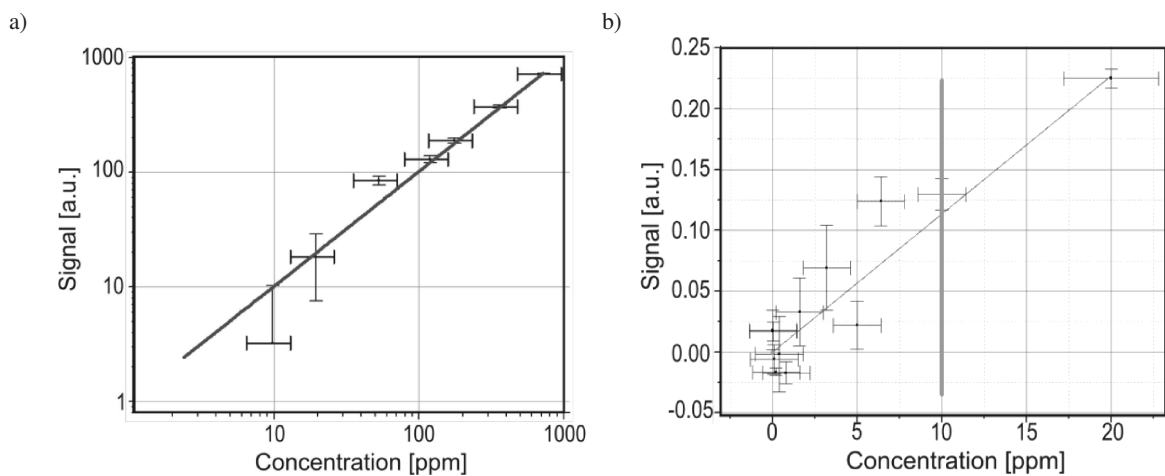


Fig. 11. Measurement of methane concentration in air: photoacoustic method (a); multipass approach (b)

Similar investigation was performed with ammonia. Wavelength of 1527.041 nm is the best for observation of this compound in NIR (Fig. 12) while absorption coefficient better than  $10^{-7} \text{ cm}^{-1}$  might be registered within this atmospheric window. The results are presented in Fig. 13.

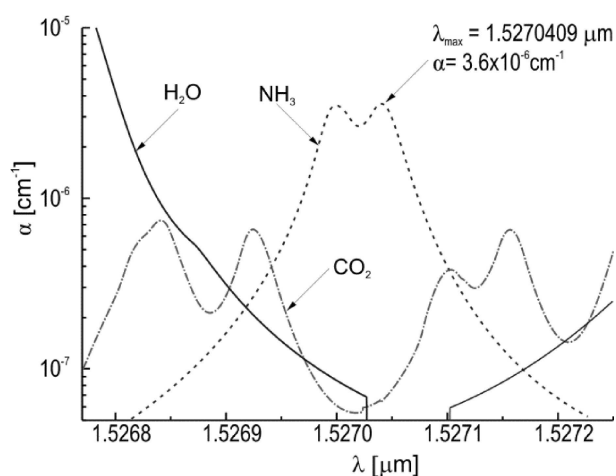


Fig. 12. Comparison of absorption spectrum of ammonia (2 ppm) with of H<sub>2</sub>O (5%) (a) and CO<sub>2</sub> (5%) (b) in the air close to the wavelength of observation

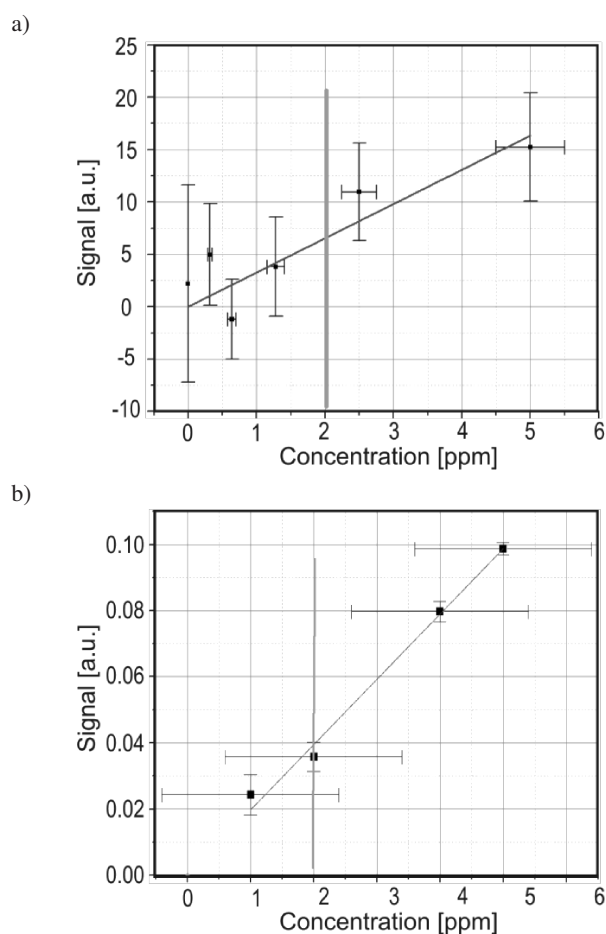


Fig. 13. Results of measurement of ammonia concentration in air: photoacoustic method (a); multipass approach (b)

The results which were presented here are very preliminary. Nevertheless it was shown that for methane and ammonia the sensitivity sufficient for health state screen monitoring was achieved even with such simple apparatus. In conclusion several improvements were noticed. PAS sensitivity might be increased one or two orders of magnitude due to rise of laser power.

MUPASS cell might be also improved several times due to application of better mirrors. Expensive wavelength meter can be replaced by a system of wavelength control and stabilization with a reference cell containing the gas of interest. Forthcoming investigation will concern detection of CO at 2333.712 nm and acetone at 266 nm. Spectral analysis provides optimistic foresees for both compounds as well. Application of CRDS for this research is also in progress.

**4.2. MIR measurements.** During experiments, the sensors operating in the mid-infrared wavelength range were also developed. Within this range, the absorption spectrum of the gases consists of series of narrow separated lines corresponding to main ro-vibronic transitions in the molecules. Therefore precise matching of the laser spectrum to selected absorption line is crucial for the sensitivity of such sensor. As it was mentioned above proper selection of the absorption lines also enables to avoid the interferences induced by other gases existing in the atmosphere. The absorption cross section as a function of wavelength for selected compounds is depicted in Fig. 14. Most of the species are important biomarkers, which were described above.

The sensors are designed for NO, N<sub>2</sub>O and for OCS detection. The simplified project of the MIR sensor is presented in Fig. 15. It consists of a laser control system, optical system, sample module and a signal processing unit. Quantum cascade lasers (Alpes Lasers SA) were applied in the optical system. Their emission lines are very narrow, and also are characterised by good spectral stability. The high detection performance of the sensor is obtained by matching wavelengths of the QC lasers radiation to the selected absorption lines of the tested gases: 5.263  $\mu\text{m}$  for NO, 5.257  $\mu\text{m}$  for OCS, and 4.529  $\mu\text{m}$  for N<sub>2</sub>O. The optical cavity was built of two concave dielectric mirrors, the reflectivity of which was approx. 0.96 at the wavelength of interest. They were located with the distance of about 60 cm. The leakage radiation from the cavities was registered with optimized detection modules – PVI-2TE (VIGO System S.A.). The main elements of the modules are MCT photodetectors, transimpedance preamplifiers and TEC units. Next, the signals from the preamplifiers were digitized using an USB AD converter (C328 series from Cleverscope).

As it was described in Sec. 2, the measurement of the absorber concentration was carried out within a two-step process. Firstly, the decay time  $\tau_0$  of lasers radiation in each optical cavity without an absorber was found. Then, the cavities were filled with the absorbing mixture and the respective decay time values  $\tau_A$  were measured. Knowing the absorption cross section  $\sigma$  of the compounds, their concentrations in respective cavities were calculated from the formula (7).



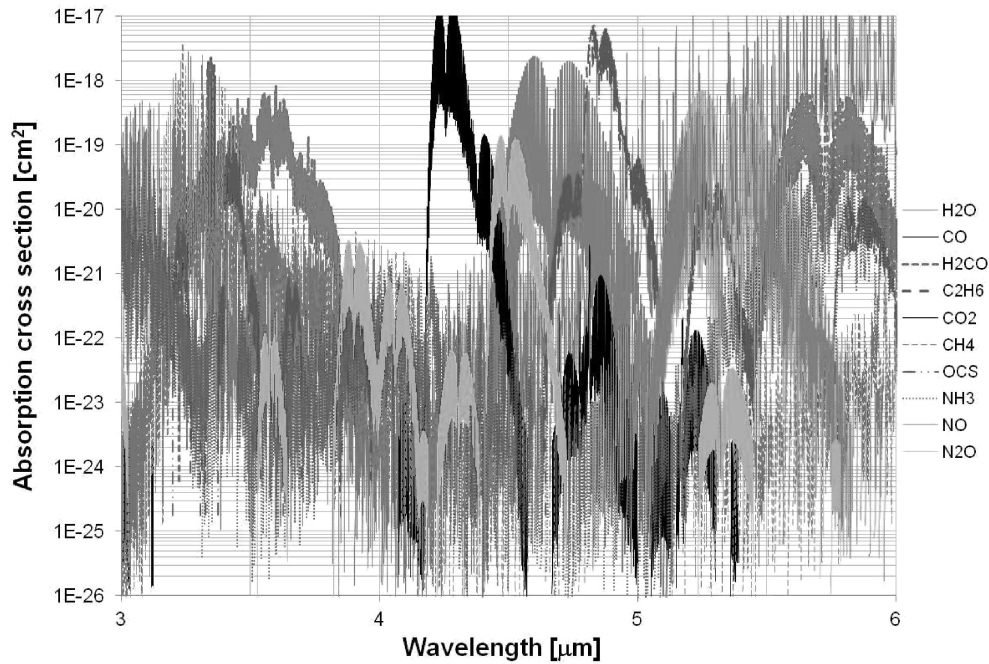


Fig. 14. Absorption cross section of the selected compounds located in 3–6  $\mu\text{m}$  region

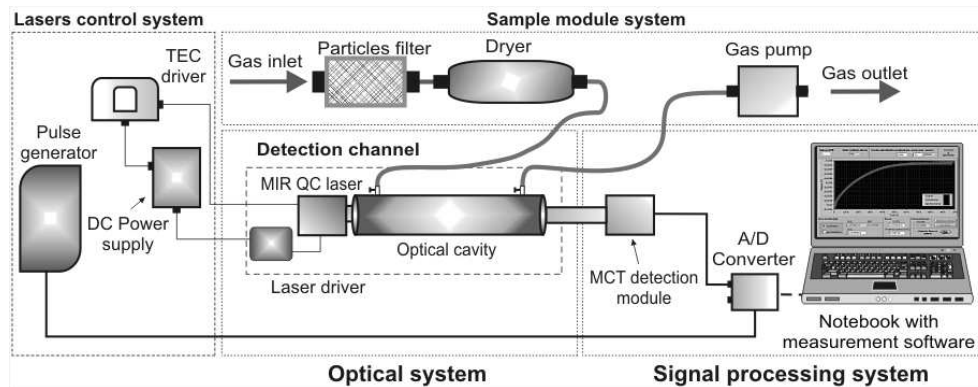


Fig. 15. Block diagram of the MIR sensor

During the sensor investigation, concentration measurements of reference gas samples were carried out. Gas samples were prepared using the 491M model gas standards generator from KIN-TEK Laboratories, Inc. (La Marque, TX, USA, Fig. 16).

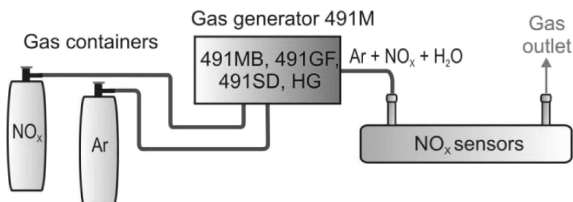


Fig. 16. Block diagram of the setup designed for NO and  $\text{N}_2\text{O}$  sensor testing

The modular construction of the instruments enables production of well controlled gas mixtures. The high precision

of the generator from a level of part per trillion (ppt) to the initial concentration of 1:1 is guaranteed. The instrument also produces both dry and moistened standard gas, which can be supplied to the sensor at an adjustable pressure. Example of the experimental results obtained during NO and OCS measurements are presented in Fig. 17.

Preliminary experiments have shown that the sensors ensure the detection of investigated gases with the limit of 35 ppb for NO, of 250 ppb for OCS and of 45 ppb for  $\text{N}_2\text{O}$  (Table 2). In case of NO and  $\text{N}_2\text{O}$  the measurements uncertainties reach the value of about 13%, while for OCS the uncertainty was 3.5% only. For nitric oxide such sensitivity is sufficient for health state screen monitoring, according ATS recommendation. However, lower detection limit can be obtained in case of OCS sensor by implementing of more powerful QCL matched to the line with higher absorption cross section, and the cavities with a higher Q-factor. Sig-

nificant improvement of the detection limits can be obtained at  $5.007 \mu\text{m}$ , where the interferences caused by  $\text{CO}_2$  and  $\text{H}_2\text{O}$  are negligible.

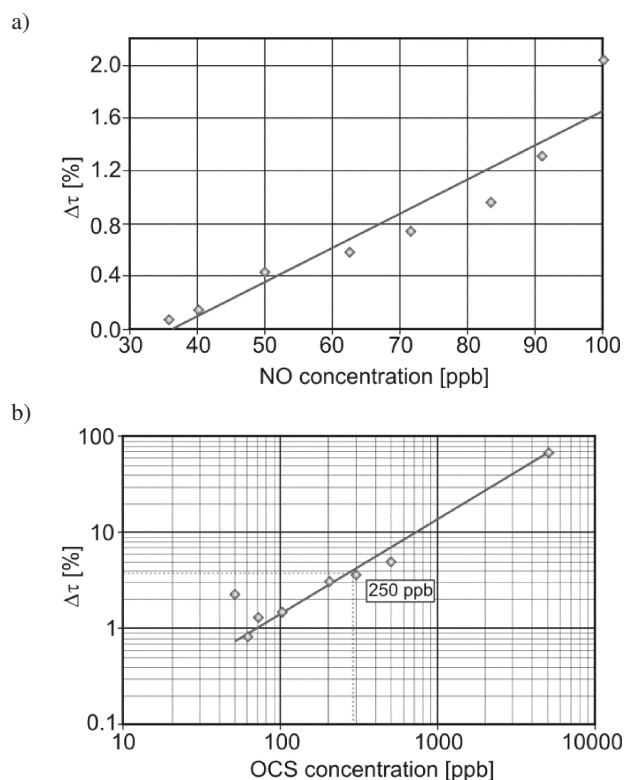


Fig. 17. Results of concentration measurements for NO (a) and OCS (b) reference samples

Table 2  
The test results of MIR sensors

Operation wavelength	Detected gas	Detection limit	Measurement uncertainty
$5.263 \mu\text{m}$	NO	35 ppb	12%
$5.257 \mu\text{m}$	OCS	250 ppb	3.5%
$4.53 \mu\text{m}$	$\text{N}_2\text{O}$	45 ppb	13%

Nitric oxide and nitrous oxide sensors can be also very useful in the case of explosives detection [39]. In combination with the system for preconcentration and thermal decomposition of investigated matter, the sensors ensure the detection of explosives such as TNT, PETN, RDX, HMX. During preliminary research 1 ng portions of the explosives were detected. The concentration of nitrous oxide varied in the range from tens to hundreds of ppb for the mentioned explosives types. In the same setup, the concentration of nitric oxide reached much higher values, even level of ppm was obtained [40].

## 5. Conclusions

The article presents an overview on the high-sensitivity laser absorption spectroscopic techniques used for trace gas detection. CRDS, MUPASS and PAS spectroscopies and various modifications of these methods combined with wavelength and frequency modulation approaches provide opportunity for

breath analysis as well as air investigation for environmental monitoring or military applications. Advantage of these techniques are the sensitivity, the selectivity, ease of use, short time of measurement, non-invasive monitoring and low operating cost. Our preliminary experiments showed that such sensors can be applied to detection of methane, ammonia, nitric oxide, nitrous oxide, and carbonyl sulfide. Quantity of these components in the exhaled air can provide the information about patient health. Progress in optoelectronics induces fast development of such sensors and in the future it would provide opportunity to construct top-table apparatus widely accessible for small medical cabinets. As a consequence the medicine would achieve the instruments for simple and non-invasive screen monitoring based on human breath analysis. Such sensors would help for early detection of cancer, diabetes, various infections, schizophrenia and other diseases.

**Acknowledgements.** This research was supported by the National Centre for Research and Development (the project SEN-SORMED – ID 179900 and the National Science Centre funds due to the DEC-2011/03/B/ST7/02544 decision.

## REFERENCES

- [1] B. Buszewski, D. Grzywiński, T. Ligor, T. Stacewicz, Z. Bielecki, and J. Wojtas, "Detection of volatile organic compounds as biomarkers in breath analysis by different analytical techniques", *Bioanalysis* 5 (18), 2287–306, doi: 10.4155/bio.13.183 (2013).
- [2] W. Gopel, J. Hessel, and J.N. Zemel, *Sensors. A Comprehensive Survey*, VCH Verlagsgesellschaft mbH, Berlin, 1995.
- [3] G.F. Fine, L.M. Cavanagh, A. Afonja, and R. Binions, "Metal oxide semi-conductor gas sensor in environmental monitoring", *Sensors* 10, 5469–5502, doi: 10.3390/s100605469 (2010).
- [4] J.S. Wilson, *Sensor Technology Handbook*, Elsevier, New York, 2005.
- [5] Kostrev, G. Wysocki, Y. Bakhirkin, S. So, M. Fraser, F. Tittel, and R.F. Curl, "Application of quantum cascade lasers to trace gas analysis", *Appl. Phys. B* 90, 165–176, doi: 10.1007/s00340-007-2846-9 (2008).
- [6] M. Murtz, "Breath diagnostics using laser spectroscopy", *Optics & Photonics News* 16, 30–35 (2005).
- [7] W. Boots, J.B.N van Berkel, J.W. Dallinga, A. Smolińska, E.F. Wouters, and F.J. van Schooten, "The versatile use of exhaled volatile organic compounds in human health and disease", *J. Breath Research* 6, 1–21, doi: 10.1088/1752-7155/6/2/027108 (2012).
- [8] J. H. Shorter, D.D. Nelson, J.B. McManus, M.S. Zahniser, S.R. Sama, and D.K. Milton, "Clinical study of multiple breath biomarkers of asthma and COPD (NO, CO<sub>2</sub>, CO and N<sub>2</sub>O) by infrared laser spectroscopy", *J. Breath Research* 5, 1–12, doi: 10.1088/1752-7155/5/3/037108 (2011).
- [9] W. Miekisch, J.K. Schubert, and G.F. Noeldge-Schomburg, "Diagnostic potential of breath analysis-focus on volatile organic compounds", *Clinica Chimica Acta* 347, 25–39, doi: 10.1016/j.cccn.2004.04.023 (2004).
- [10] C.D.R. Dunn, M. Black, D.C. Cowell, C. Penault, N.M. Ratcliffe, R. Spence, and C. Teare, "Ammonia vapour in the mouth as a diagnostic marker for Helicobacter pylori infection: pre-

- liminary 'proof of principle' pharmacological investigations", *British J. Biomedical Science* 58, 66–75 (2001).
- [11] S.S. Sehnert, L. Jiang, J.F. Burdick, and T.H. Risby, "Breath biomarkers for detection of human liver diseases: preliminary study", *Biomarkers* 7, 174–187, doi: 10.1080/13547500110118184 (2002).
- [12] M.R. McCurdy, Y. Bakhirkin, G. Wysocki, R. Lewicki, and F.K. Tittel, "Recent advances of laser-spectroscopy-based techniques for application in breath analysis", *J. Breath Res.* 1, 014001, doi: 10.1088/1752-7155/1/1/014001 (2007).
- [13] Ch. Wang and P. Sahay, "Breath analysis using laser spectroscopic techniques: breath biomarkers, spectral fingerprints, and detection limit", *Sensors* 9, 8230–8262, doi: 10.3390/s91008230 (2009).
- [14] A. Wehinger, A. Schmid, S. Mechtcheriakov, M. Ledochowski, C. Grabmer, A. Guenther, G.A. Gastl, and A. Amann, "Lung cancer detection by proton transfer reaction mass-spectrometric analysis of human breath gas", *Int. J. Mass Spectrom.* 265, 49–59, doi: 10.1016/j.ijms.2007.05.012 (2007).
- [15] S.E. Ebeler, A.J. Clifford, and T. Shibamoto, "Quantitative analysis by gas chromatography of volatile carbonyl compounds in expired air from mice and human", *J. Chromatogr. Biomed. Sci. Appl.* 702, 211–5, doi: 10.1016/S0378-4347(97)00369-1 (1997).
- [16] F. Schmidt, "Laser-based absorption spectrometry, development of nice-ohms towards ultra-sensitive trace species detection", *Doctoral Thesis*, Umea University, Umea, 2007.
- [17] L.S. Rothman, D. Jacquemart, and A. Barbe, "The HITRAN 2004 molecular spectroscopic database", *J. Quant. Spectrosc. Ra.* 96, 139–204, doi: 10.1016/j.jqsrt.2004.10.008 (2005).
- [18] W. Demtröder, *Laser Spectroscopy. Basic Concepts and Instrumentation*, Springer, Berlin, 2003.
- [19] M. Bugajski, K. Kosiel, A. Szerling, J. Kubacka-Traczyk, I. Sankowska, P. Karbownik, A. Trajnerowicz, E. Pruszyńska Karbownik, K. Pierściński, and D. Pierścińska, "GaAs/AlGaAs ( $\sim 9.4 \mu\text{m}$ ) quantum cascade laser operating at 260K", *Bull. Pol. Ac.: Tech.* 58 (4), 471–476, doi: 10.2478/v10175-010-0045-z (2010).
- [20] G. Berden, R. Engeln, *Cavity Ring-Down Spectroscopy: Techniques and Applications*, Wiley-Blackwell, London, 2009.
- [21] K.W. Busch and M.A. Busch, *Cavity-Ringdown Spectroscopy An Ultratrace-Absorption Measurement Technique*, American Chemical Society, New York, 1999.
- [22] <http://www.chem.ualberta.ca/~xu/research/crds1.jpg>
- [23] J.M. Herbelin, J.A. McKay, M.A. Kwok, R.H. Ueunten, D.S. Urevig, D.J. Spencer, and D.J. Benard, "Sensitive measurement of photon lifetime and true reflectances in optical cavity by a phase-shift method", *Applied Optics* 19 (1), 144–147, doi: 10.1364/AO.19.000144 (1980).
- [24] F.K. Tittel, G. Wysocki, A. Kostrev, and Y. Bakhirkin, "Semiconductor laser based trace gas sensor technology: recent advances and application", in *Mid-infrared Coherent Sources and Applications*, eds. M. Ebrahim-Zaden and I.T. Sorokina, pp. 467–493, Springer, Berlin, 2007.
- [25] D. Romanini, A.A. Kachanov, J. Morville, and M. Chenevier, "Measurement of trace gases by diode laser cavity ringdown spectroscopy", *Proc. SPIE* 3821, 94–104, doi:10.1117/12.364170 (1999).
- [26] R.W.P. Drever, J.L. Hall, F.V. Kowalski, J. Hough, G.M. Ford, A.J. Munley, and H. Ward, "Laser phase and frequency stabilization using an optical resonator", *Appl. Phys. B* 31 (2), 97–105 (1983).
- [27] A. Cygan, D. Lisak, S. Wójtewicz, J. Domysławska, J.T. Hodges, R.S. Trawinski, and R. Ciuryło, "High signal-to-noise ratio laser technique for accurate measurements of spectral line parameters", *Phys. Rev. A* 85, 022508, doi: 10.1103/PhysRevA.85.022508 (2012).
- [28] J. Wojtas, Z. Bielecki, T. Stacewicz, J. Mikołajczyk, and M. Nowakowski, "Ultrasensitive laser spectroscopy for breath analysis", *Opto-Electron. Rev.* 20 (1), 26–39 (2012).
- [29] Y.A. Bakhirkin, A.A. Kostrev, R.F. Curl, F.K. Tittel, D.A. Yarekha, I. Hvozdar, M. Giovannini, and J. Faist, "Sub-ppbv nitric oxide concentration measurements using cw thermoelectrically cooled quantum cascade laser-based integrated cavity output spectroscopy", *Appl. Phys. B* 82, 149–154, doi:10.1007/s00340-005-2058-0 (2006).
- [30] [http://www.ru.nl/tracegasfacility/trace\\_gas\\_research/spectroscopic/cavity-enhanced/](http://www.ru.nl/tracegasfacility/trace_gas_research/spectroscopic/cavity-enhanced/)
- [31] M. Murtz, B. Frech, and W. Urban, "High-resolution cavity leak-out absorption spectroscopy in the  $10\mu\text{m}$  region", *Appl. Phys. B* 68, 243–249, doi: 10.1007/s003400050613 (1999).
- [32] D. Halmer, G. von Basum, P. Hering, and M. Murtz, "Mid-infrared cavity leak-out spectroscopy for ultrasensitive detection of carbonyl sulfide", *Optics Letters* 30 (17), 2314–2316, doi: 10.1364/OL.30.002314 (2005).
- [33] T. Starecki, *Selected Aspects of Photoacoustic Devices*, BTC, Legionowo, 2009, (in Polish).
- [34] T. Kuusela and J. Kauppinen, "Photoacoustic gas analysis using interferometric cantilever microphone", *Appl. Spectrosc. Rev.* 42, 443, doi: 10.1080/00102200701421755 (2007).
- [35] L. Dong, A. Kostrev, D. Thomazy, and F.K. Tittel, "Compact portable QEPAS Multi-gas sensor", *Proc. SPIE* 7945, 79450R-1, doi: 10.1117/12.875108 (2011).
- [36] A. Kachanov, S. Koulikov, and F.K. Tittel, "Cavity-enhanced optical feedback-assisted photo-acoustic spectroscopy with a 10.4 lm external cavity quantum cascade laser", *Appl. Phys. B* 110, 47–56, doi: 10.1007/s00340-012-5250-z (2013).
- [37] M. McCurdy, Y. Bakhirkin, G. Wysocki, R. Lewicki, and F.K. Tittel, "Recent advances of laser-spectroscopy based techniques for applications in breath analysis", *J. Breath Res.* 1, doi:10.1088/1752-7155/1/1/014001, 014001 (2007).
- [38] Ch. Wang and A. Mbi, "A new acetone detection device using cavity ringdown spectroscopy at 266 nm: evaluation of the instrument performance using acetone sample solutions", *Meas. Sci. Technol.* 18, doi:10.1088/0957-0233/18/8/051, 2731–2741 (2007).
- [39] T. Pustelny, M. Procek, E. Maciak, A. Stolarczyk, S. Drewniak, M. Urbańczyk, M. Setkiewicz, K. Gut, and Z. Opilski, "Gas sensors based on nanostructures of semiconductors ZnO and TiO", *Bull. Pol. Ac.: Tech.* 60 (4), doi: 10.2478/v10175-012-0099-1, 853–860 (2012).
- [40] J. Wojtas, T. Stacewicz, Z. Bielecki, B. Rutecka, R. Medrzycki, and J. Mikołajczyk, "Towards optoelectronic detection of explosives", *Opt. Electron. Rev.* 21, doi: 10.2478/s11772-013-0082-x, 9–18 (2013).